AIAA JOURNAL
Vol. 34, No. 12, December 1996

Experimental Studies of Magnetic Levitation Train Aerodynamics

J. S. Tyll,* D. Liu,* J. A. Schetz,† and J. F. Marchman‡
Virginia Polytechnic Institute and State University, Blacksburg, Virginia 24061-0203

A high-speed moving-track test system was designed and built for the aerodynamic testing of magnetically levitated vehicle (Maglev) models. The moving-track test system was configured to match wind speeds up to 150 miles per hour and to extend a sufficient distance upstream and downstream of the test-vehicle model to provide a uniform flowfield at the model nose and to simulate proper closure of the flowfield at the rear of the model. Extensive flowfield testing around the track system confirmed its capability to properly simulate the flow around the high-speed tracked vehicle. The selected Maglev model was tested with the moving-track system, and aerodynamic forces and moments were measured. Hot-wire anemometer surveys were used to examine the flowfield behind the model and the turbulence levels and transition location on the vehicle nose. Flow visualization tests were also conducted to verify the nature of the flowfield found in the velocity surveys. Testing included direct measurement of skin friction at selected locations on the model. Separate tests were conducted with the track system removed from the tunnel. The resulting data provide a database for use in the design of Maglev systems and for comparison with computer analyses.

Introduction

MAGNETICALLY levitated (Maglev) vehicles have been proposed as a means of high-speed ground transportation for over 50 years. Research was conducted in Germany in the 1930s, and Hermann Kemper received a patent on a Maglev system design in 1934.[1] In 1965, the U.S. Congress passed the High Speed Ground Transportation Act, funding research through 1972.[2] Interest in Maglev was spurred by the crowded U.S. air transportation system and, in 1991, President George Bush signed the Intermodal Surface Transportation Efficiency Act into law. Early programs developed in response to this act centered primarily around the complex problems of magnetic levitation, propulsion, and track system design needed for the development of a successful Maglev system. Meanwhile, in France, Germany, Japan, and Korea, full-scale test and demonstration systems have already been put into operation.

Aerodynamic drag is important for any high-speed vehicle, and the mechanisms causing drag are often more complex for ground vehicles than for aircraft. The aerodynamic forces resulting from vehicle proximity to the ground, roadway, or track are difficult to predict or determine in conventional wind tunnels. The need for moving ground, roadway, or track simulations in wind-tunnel testing has been debated extensively for such vehicles as cars and trains.

Maglev vehicles offer one advantage over other forms of ground transport in their elimination of the friction and aerodynamic loads resulting from any form of wheel/surface contact. This is the primary reason for their assumed capability of exceeding the top speeds of current high-speed trains by as much as 100 miles per hour (mph). Although the absence of wheels does eliminate a source of friction drag, it does not reduce the complexity of predicting or measuring aerodynamic drag due to the flow in the vehicle–track interface region. Measurement of such aerodynamic loads in wind-tunnel tests, in fact, is complicated further by the way that many Maglev vehicles wrap around a track, necessitating not only the proper simulation of track motion but also of the flow under the track. For this and other reasons, a specially designed moving-belt track system is needed for wind-tunnel tests of Maglev vehicle aerodynamics.

Presented as Paper 95-1917 at the 13th Applied Aerodynamics Conference, San Diego, CA, June 19–22, 1995; received Sept. 13, 1995; revision received June 18, 1996; accepted for publication Aug. 23, 1996; also published in *AIAA Journal on Disc*, Volume 2, Number 1.

*Graduate Student, Aerospace and Ocean Engineering Department. Student Member AIAA.

†J. Byron Maupin Professor, Aerospace and Ocean Engineering Department. Fellow AIAA.

‡Professor and Assistant Department Head, Aerospace and Ocean Engineering Department. Associate Fellow AIAA.

The wind-tunnel test facility for testing of Maglev vehicle models is a single-return facility with a very low freestream turbulence level and a 6 × 6 × 24 ft test section. This is long enough to enable proper upstream and downstream simulation for an approximately one-twelfth-scale model of a Maglev vehicle and its track. This vehicle design uses the electromagnetic suspension (EMS) attracting-magnetic-force system where the vehicle undercarriage wraps around the track as shown in Fig. 1, as opposed to the electrodynamic suspension, magnetically repelling system where the vehicle rides within a trough type of track. The primary test objective was to determine experimental values of aerodynamic load and moment coefficients that could be used for comparison with computational predictions.

High-Speed Track System

The first task was the design of a high-speed Maglev track simulation system. The use of moving-belt systems in wind tunnels for proper simulation of vehicle–ground interactions is fairly common; however, the usual system employs a belt that replaces the tunnel floor. In the present case, the test vehicle was to be wrapped around the moving track rather than merely being situated above a moving ground plane. It was therefore important that the moving belt be placed well into the test section and that the flow under the belt (track) be as near to freestream conditions as possible. The top speed of the wind tunnel is about 175 mph and one track system design goal was to use a belt that would move as near to this speed as possible to maximize the Reynolds numbers. Another parameter, track or belt width, was determined by wind-tunnel blockage considerations that dictated a roughly 1-ft^2 Maglev model cross section. This resulted in the specification of a 6-in. belt width. A 6-ft length was selected for the Maglev wind-tunnel model and, to allow enough upstream

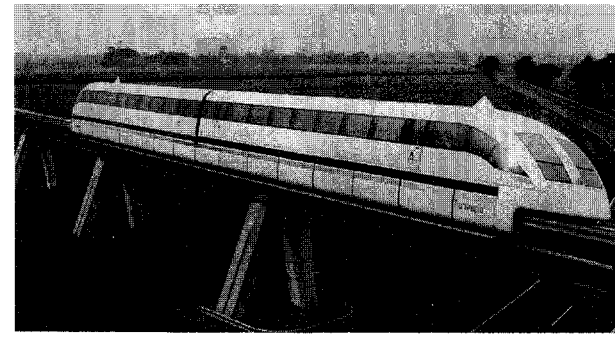

Fig. 1 Transrapid 06, an EMS Maglev system.

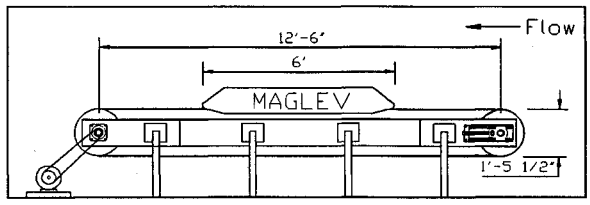

Fig. 2 Design for track system.

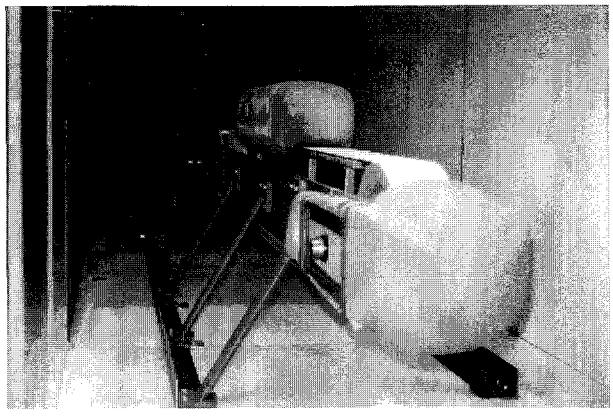

Fig. 3 Track system and model in stability tunnel.

length for a uniform flowfield to properly develop at the nose of the model and enough downstream length to allow proper simulation of the closure of the vehicle wake, the track system length was set at approximately three times the model length. The resulting design is shown in Fig. 2.

This moving-track system was designed to place the test-vehicle model in the center of the test section vertically and horizontally, with the model suspended from a strut through the wind-tunnel ceiling. The system was driven by an electric motor and belt–pulley system. The side supports were streamlined aircraft strut extrusions.

Two primary concerns emerged regarding the moving-belt system design. Several belt and pulley manufacturers expressed concern about running any belt at the desired speeds, and there were serious questions about the influence of such a large system on the flowfield seen by the model. Only one company could meet the design requirements. They designed a special continuous belt and manufactured the pulleys for the system.

While the belt and pulleys for the system were being manufactured, a small, one-twelfth-scale model of the moving-track system was built and mounted on a ground board for testing in the department's 3-ft-diam, open-test-section wind tunnel. This small, working model of the track system was used to get a first look at the flowfield around the system and to investigate various methods for shrouding and streamlining the system to create the desired uniform flow at the point on the belt where the nose of the model would be placed.

Tests with this model system were conducted at tunnel and belt speeds of 91 fps (28 m/s), the top speed for the small belt drive motor. The resulting flowfield was evaluated using a tuft grid, pitot tube surveys, and hot-wire anemometer surveys. These tests, reported by the two undergraduate students who made the model and ran the tests,[3] showed a surprisingly uniform flow in the vicinity of the proposed Maglev nose location with the belt running, even without any attempts at belt system streamlining or shrouding. There was some evidence of flow separation around the front of the belt system and, although the moving belt was apparently successful at forcing reattachment, the resulting turbulence levels were larger than desired. Hence, several different nose shroud shapes were proposed for investigation. Also, some nonuniformities in the flow along the side of the system led to a desire to attempt some streamlining of the area behind the pulley mounts.

The best combination of belt-system nose shroud and bearing block streamlining found in the small tunnel tests resulted in an improved uniformity of flow along the sides of the system and a significant reduction in the turbulence measured over the belt.[3] These shapes were then scaled up to the full-size test track dimensions and adapted to that test system, as shown in Fig. 3.

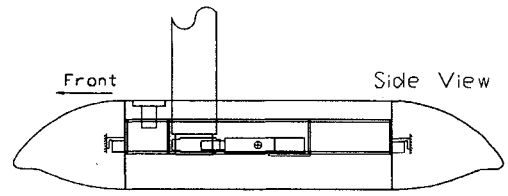

Fig. 4 Design for Maglev model.

Maglev Model

The wind-tunnel test-model geometry was based on a design furnished by the Northrop–Grumman Corporation. The model was constructed in three sections with the center section designed to house a six-component strain-gauge balance that would attach to a specially designed mounting strut hung from the tunnel ceiling (Fig. 4). The center section was built of wood and plastic foam with an internal aluminum frame attached to the balance. Identical nose and tail sections were formed from plastic foam. The nose and tail pieces, attached to the center section via a load cell, were used to make independent measurements of the forces on the nose and tail. The model was designed to allow for pressure taps and to accommodate special skin friction balances at selected locations.

Testing

Prior to actual wind-tunnel testing, extensive studies were conducted to determine the dynamic behavior of the belt at high speed and to investigate any control problems associated with belt acceleration and deceleration. Of special concern was out-of-plane belt motion that might lead to belt contact with the Maglev model. Such contact would result in false force and moment measurements and would damage the model and belt.

The test program included runs in which the flowfield was cataloged with only the track system in the test section. This was followed by testing with the Maglev model in place on the track system and an investigation of the flows around the model. Hot-wire anemometer measurements were used to determine velocities and turbulence levels at selected locations. These tests included an examination of the flow around the model nose with and without boundary-layer tripping. Trip location was determined from information provided by Northrop–Grumman and calculations done at Virginia Tech. Flow visualization tests also were run using fine nylon tufts attached to the Maglev model.

The remaining wind-tunnel tests consisted of force-and-moment-measurement test runs and runs made with a skin friction balance mounted in the top of the model. Final force and moment tests were run after the moving-belt track system was removed from the test section to give an understanding of the effects of the model–track interaction.

Test Results

The purpose of the first tests conducted was to ascertain the nature of the flowfield around the belt–track system in the vicinity of the Maglev model location. Velocity profiles and turbulence profiles were measured over the belt and on both sides of the belt, both with the belt moving and with it stationary. This was done at two primary locations, at the point where the Maglev model nose would be located and at the tail position. Sample test results are shown in Figs. 5 and 6.

Figures 5 and 6 present a larger-scale view of the velocity and turbulence profiles at the model nose location. These plots show both belt centerline data and the results of surveys on both sides of the belt. In Fig. 5, the data for the case with the stationary belt indicate that both velocity and flow turbulence off to the sides of the belt were fairly uniform from a point about 5 in. below the belt to almost 20 in. above the belt. The belt centerline plots show that the velocity and turbulence boundary layers are relatively small.

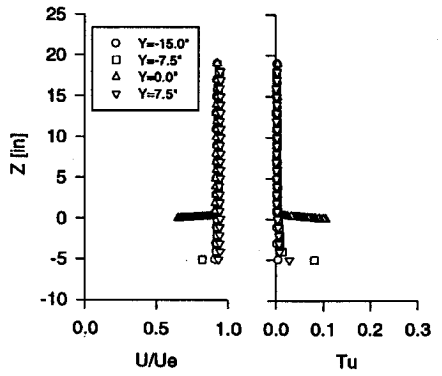

Fig. 5 Nose location, stationary-belt-region velocity and turbulence profiles.

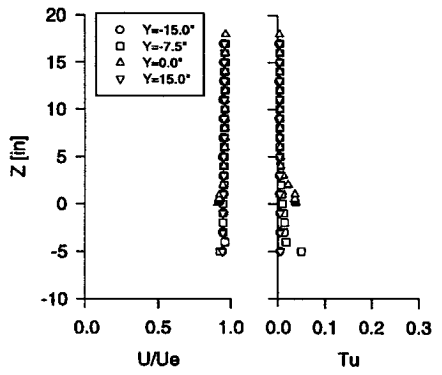

Fig. 6 Nose location, moving-belt velocity and turbulence profiles.

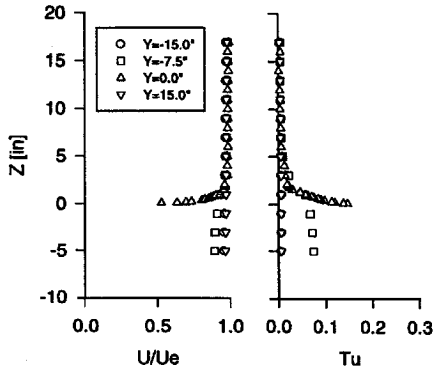

Fig. 7 Tail location, stationary-belt velocity and turbulence profiles.

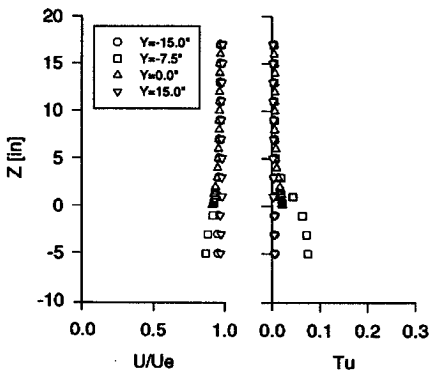

Fig. 8 Tail location, moving-belt velocity and turbulence profiles.

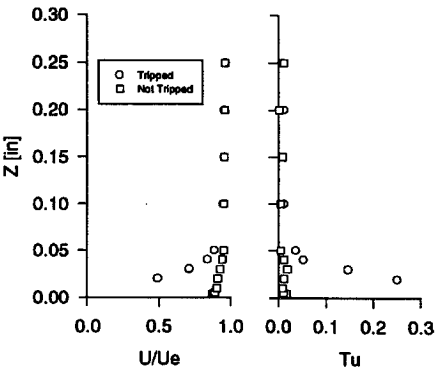

Fig. 9 Boundary-layer data behind trip location.

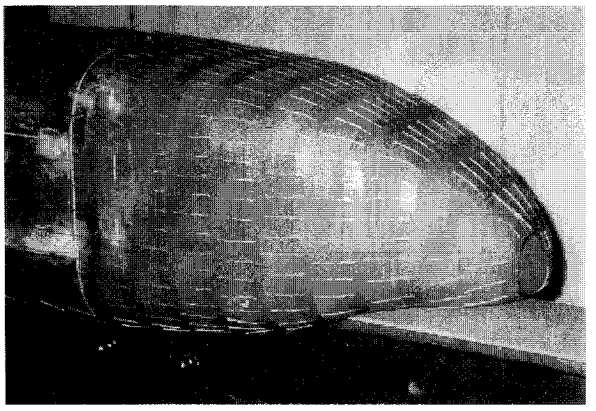

Fig. 10 Tuft photo of Maglev nose.

Figure 6 shows similar plots for the case with the moving belt. These data indicate an even more uniform velocity to the side of the belt system than seen in Fig. 5, but show an increased level of turbulence extending 2 to 3 in. into the region above the belt centerline. There is increased turbulence below the level of the track surface.

Figures 7 and 8 present boundary-layer information similar to that of Figs. 5 and 6 but at a location where the tail of the Maglev model would be. Note that the stationary-belt boundary layer has grown in height and the turbulence levels have increased. There is an indication of a slight reduction in velocity near the belt surface in the moving-belt case, but the turbulence levels are uniform and reduced from those at the model nose location. The velocity and turbulence profiles at this location show results similar to their upstream counterparts except for the larger boundary layer in the stationary-belt case (Fig. 7) and a larger increase in turbulence level below the belt height in both cases (Figs. 7 and 8). A velocity deficit also has built up below the belt in both cases. This undoubtedly is due to the buildup of a boundary layer on the supporting I-beam structure. The development of a small velocity deficit and turbulence increase at the center of the moving belt at this location is also evident in Fig. 8.

Similar flowfield surveys were made at the streamwise center of the belt, coinciding with the location of the midpoint of the Maglev model. These gave results that are consistent with the two model end locations.

After the Maglev model was placed on the test system in the tunnel and tests were conducted to ensure correct alignment of the model with the track, boundary-layer surveys were run near the nose of the model to measure the effectiveness of boundary-layer tripping. Figure 9 shows the boundary-layer velocity profile and turbulence profile at a point just aft of the trip location measured before and after the trip was installed. The trips produced a turbulent boundary layer.

To get a better understanding of the nature of the flow around the model, the model was tufted with small nylon thread strips. Figures 10 and 11 show the nose and tail of the Maglev model with the wind tunnel and track system operating. Figure 10 shows the model boundary-layer trip location and reveals a well-behaved, smooth flow over most of the model. Some vortical activity is evident

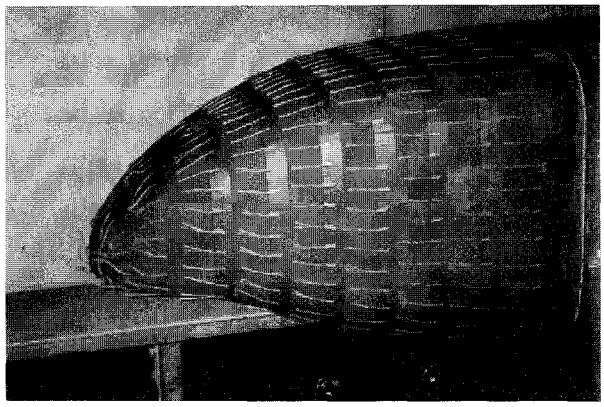

Fig. 11 Tuft photo of Maglev tail.

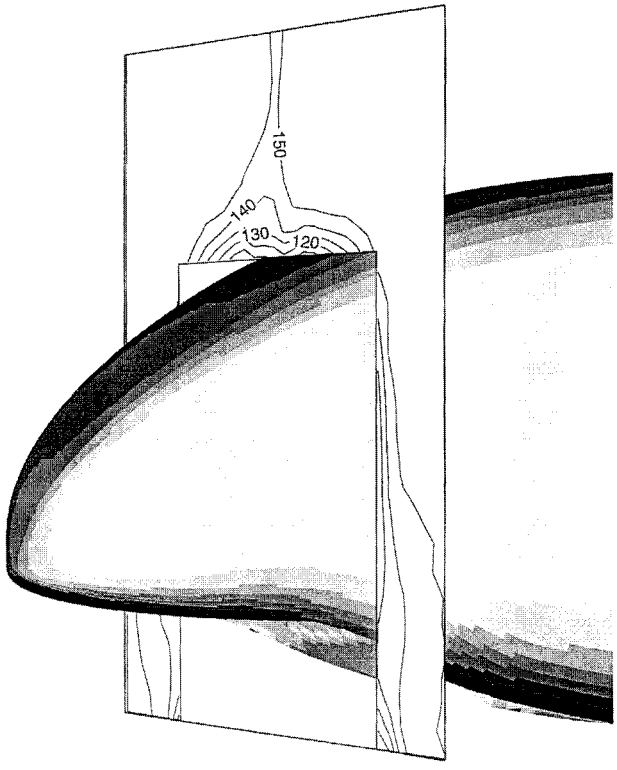

Fig. 12 Velocity contours near track exit slot.

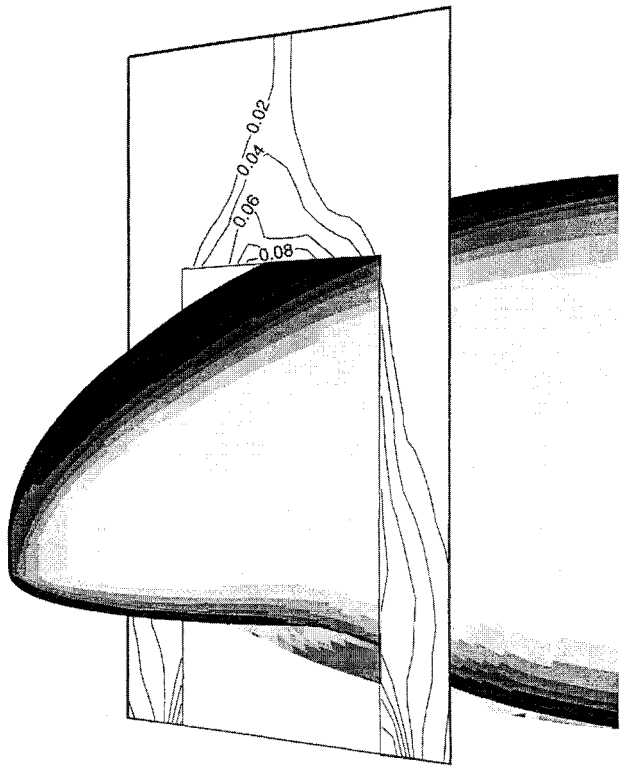

Fig. 13 Turbulence contours near track exit slot.

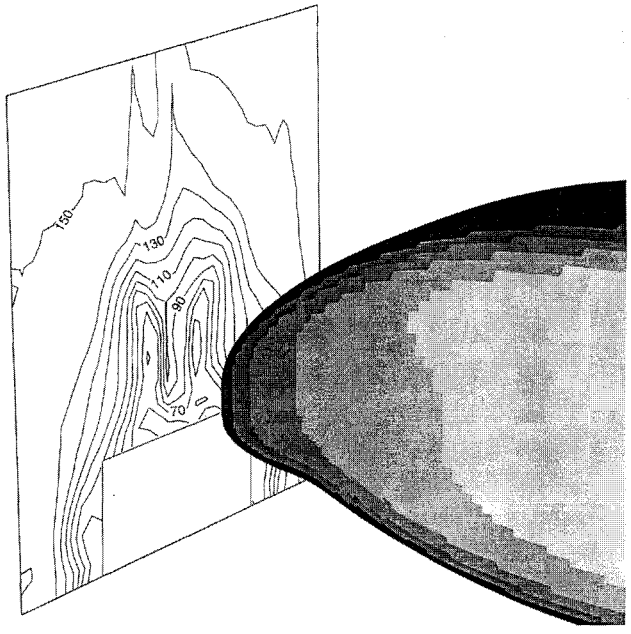

Fig. 14 Velocity contours aft of tail.

in the corner radius area at the base of the model downstream of the edge of the track entry slot. One would expect the flow in this region to exhibit some complex flow behavior. These tests confirm that expectation and suggest that more detailed studies of the flows in the immediate vicinity of the track entry slot might be desirable.

The flow around the model tail is seen to remain well behaved over much of the surface. Separation appears evident at the end of the vehicle and seems to begin farther upstream along the base of the model than on top. Judging from this, one might question the use of an identical shape for the Maglev nose and tail as the optimum configuration, because different nose and tail shapes might result in flow improvement. This Maglev configuration was designed with identical nose and tail sections to avoid the need to turn the vehicle around at the end of a track for the return journey.

Flowfield surveys were conducted near the track exit slot and at a location just downstream of the model to get a better look at the wake. These hot-wire anemometer measurements of velocity and turbulence levels are shown in Figs. 12–15. Figures 12 and 13 show contours of velocity and turbulence level, respectively, for a survey in the track exit slot region of the model. It is evident that flow speed is decreasing and turbulence levels are increasing primarily over the rapidly sloping upper surface of the model and in the track exit and base region. There is no indication of actual flow separation at this point because the lowest speeds indicated are about two-thirds of the freestream value; however, the tendency for later separation is evident. One will also note a thin vertical region of slightly reduced velocity and increased turbulence above the model. This is the result of a very thin wake from the model support strut.

Figures 14 and 15 present the velocity and turbulence-level profiles just downstream of the model tail. Both plots show a distinct area of turbulent wake behind the model, which is most intense in vertical regions to either side of the model centerline, connected by a horizontal region just above the track location. Comparing these

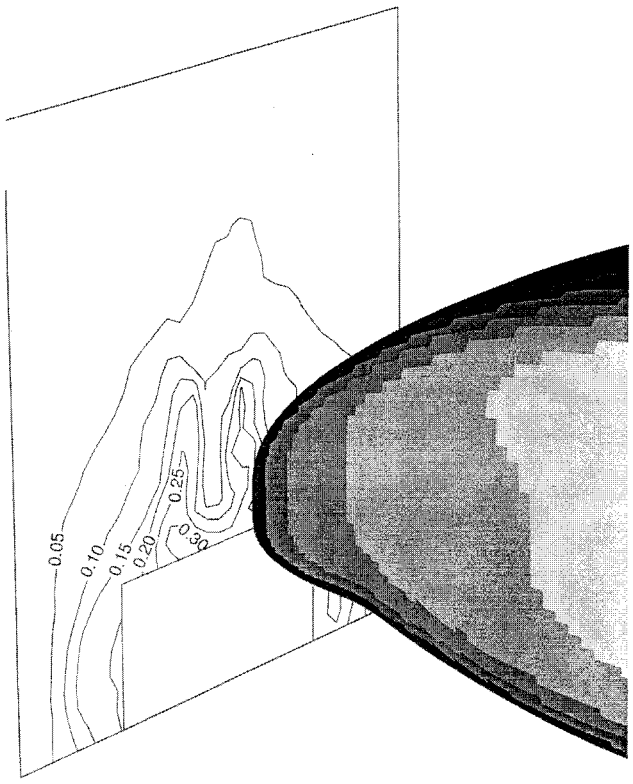

Fig. 15 Turbulence contours aft of tail.

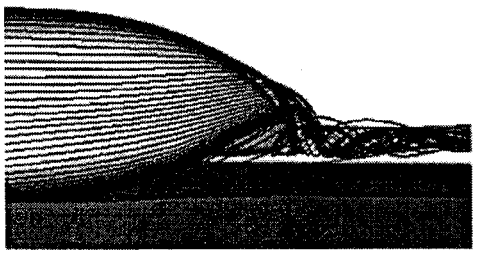

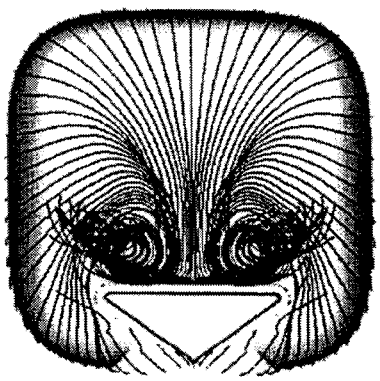

Fig. 16 Computed flow from Ref. 4.

profiles with the flow visualization in Fig. 11 suggests vortical flows coming primarily from the base of the vehicle and moving up over the sides to form the wake shown in the figures. Also note that the wake from the model support strut appears to have little, if any, influence on the model separation process.

These measured velocity and turbulence profiles aft of the Maglev model compare favorably to the flow pattern computed by Siclari and Ende,[4] shown in Fig. 16. There is very good agreement with the vortex locations shown in Fig. 16 and the profiles seen in Fig. 14.

The ultimate goal of this research was to measure forces and moments on the Maglev model. The wind tunnel's ST-01, six-

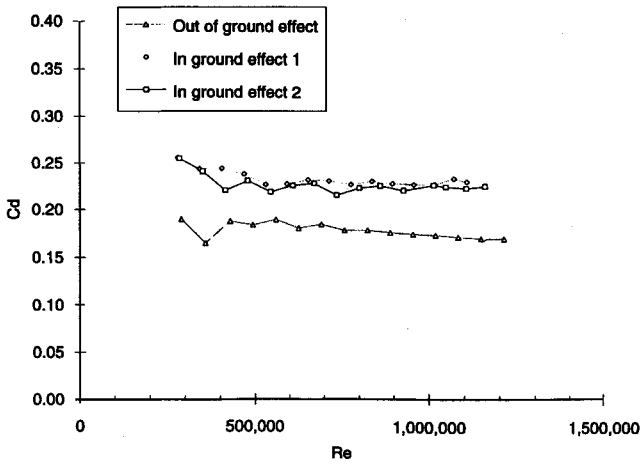

Fig. 17 Drag coefficient relative to Reynolds number.

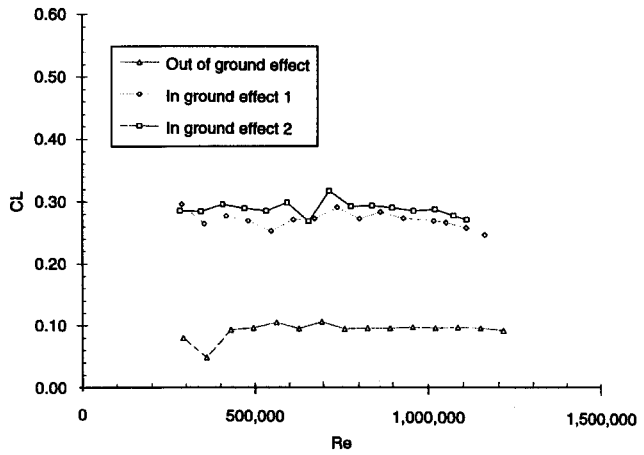

Fig. 18 Lift coefficient relative to Reynolds number.

component strain-gauge balance was used for these measurements, and the results are shown in Figs. 17–19. Force and moment measurements were made for a range of Reynolds numbers from 2×10^5–1.2×10^6 based on the 1-ft cross-sectional dimension of the model. Lift and drag coefficient data were computed using the model frontal area of 0.82 ft^2 as the reference, and the pitching moment coefficient was calculated using the frontal area and the 1-ft cross-sectional dimension for reference. The data presented in the following figures are for two experimental configurations, the model with moving belt and the model suspended in an otherwise empty test section.

Figure 17 shows the drag coefficient (C_d) to decrease very slightly with increasing Reynolds number. The fact that there is almost no Reynolds number sensitivity over this range indicated that the boundary-layer trip was successful. In the 10^6 Reynolds number range, the C_d values are about 0.17 for the model with no test track and 0.24 with the moving track. These results point out the importance of including the moving-track simulation in any analysis, experimental or analytical, of the aerodynamics of Maglev systems. Basing drag predictions on vehicle-only data or computations can lead to 40% or higher error.

Figure 18 presents the lift coefficient (C_L) data for the same cases. The data show that C_L is almost tripled by the presence of the moving-belt system over that for the model suspended in the otherwise empty test section. The model alone in the tunnel produced a C_L of around 0.08, whereas with the moving belt track it produced a C_L of approximately 0.22. This obviously is due to the dramatic alteration of the flow under the model by the presence of the track and the belt motion.

The pitching moment results are shown in Fig. 19. All measured values were negative or nose down. The pitching-moment coefficient showed little variation with Reynolds number when the Maglev model was tested in the empty test section; however, with the moving

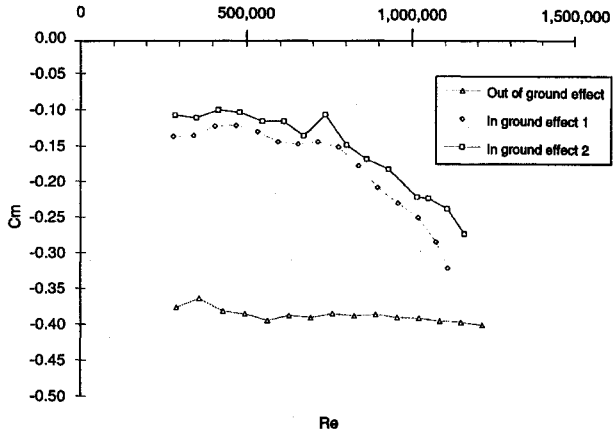

Fig. 19 Pitching-moment coefficient relative to Reynolds number.

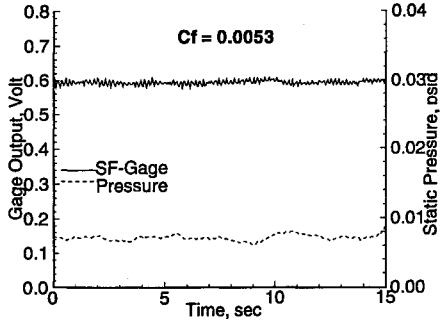

Fig. 20 Skin friction gauge output.

belt there was an increase in the nose-down coefficient (decrease in C_m) with increasing Re.

Skin Friction Measurements

A knowledge of the level of skin friction at various points on the vehicle is important in assessing the sources of drag that contribute to the total drag measured by the wind-tunnel balance system. To determine this skin friction level, direct local measurements are being made on the Maglev model by using a floating head balance. The 1.5-in.-diam floating-head surface was mounted on the top of the Maglev model center section, just aft of the nose section, as shown in Fig. 4. In future tests, this balance will be mounted with its floating surface under the model above the moving belt to direct particular attention to the skin friction levels in that gap.

The frictional force on the floating head of the skin friction balance is determined with a semiconductor strain gauge on a cantilever beam that supports the head. A typical balance output trace is shown in Fig. 20. In this trace, it can be seen that the output remains quite constant with little oscillation. The 0.0053 value for the skin friction coefficient was calculated using the measured wall shear and the freestream velocity. In later test work, the inviscid velocity at the boundary-layer edge at the gauge location will be measured and used in the skin friction coefficient calculation. This will yield a lower value of the coefficient.

Conclusions

A high-speed, moving-belt, wind-tunnel track system was successfully developed for the testing of Maglev models at speeds sufficient to determine full-scale Maglev vehicle aerodynamic behavior. Wind-tunnel tests of the track system showed that the work done on an earlier, smaller-scale track model was successful in giving a realistic, uniform flowfield in which to test a tracked Maglev vehicle. Test results for the baseline model gave a drag coefficient of 0.24 with the moving track system and 0.17 on the free vehicle. These values fall in the general range of drag coefficient values published on similar ground and tracked vehicle shapes. The total drag measured by the balance can be taken as consisting of frictional drag, pressure or form drag, and drag due to lift.

The flow patterns observed in tuft tests and measured at various locations compare favorably with the computed flows, which also have vortices forming on the underside of the vehicle and counter-rotating vortices near the track exit slot at the Maglev tail.

Wind-tunnel testing of this and other Maglev vehicle designs is continuing at Virginia Tech. The moving-track system developed for these tests is adaptable to a wide range of vehicle shapes. Current test plans include studies of two additional designs. Future tests also will include detailed pressure distribution measurement, independent measurement of the forces on vehicle model nose and tail sections, and direct measurement of skin friction at numerous locations on the models. The test results will provide a much needed database for current and future Maglev design and development programs.

Acknowledgments

The authors would like to thank NASA Langley Research Center (Grant NAS1-19610-16) and the Federal Railway Administration (FRA) for their support of this research. Special thanks go to Technical Advisor Dennis Bushnell of NASA, Technical Advisor Jim Milner of the FRA, and Mike Siclari of Northrop–Grumman Corporation for their suggestions and support. Maglev vehicle designs were provided by Northrop–Grumman Corporation.

References

[1]Dickhart, W. W., III, "The Transrapid Maglev System—an Update," Society of Automotive Engineers, SAE Paper 921583, Warrendale, PA, Aug. 1992.

[2]Wyczalek, F. A., "Preface," *MAGLEV*, SP-926, Society of Automotive Engineers, Warrendale, PA, 1992.

[3]Valdivia, A., and Wilt, J., "Analysis of Moving Ground Plane Aerodynamics for Development of a MAGLEV Test Apparatus," AIAA Mid-Atlantic Student Conf., Hampton, VA, April 1995.

[4]Siclari, M., and Ende, R., "The Application of Navier–Stokes Computations to the Design of High-Speed/Low Drag Magnetically Levitated (Maglev) Vehicle Shapes," AIAA Paper 95-1908, June 1995.